Some Aspects of the Mechanical Response of BMI 5250-4 Neat Resin at 191°C: Experiment and Modeling

M. B. Ruggles-Wrenn, J. G. Balaconis

Department of Aeronautics and Astronautics, Air Force Institute of Technology, Wright-Patterson Air Force Base, Ohio 45433-7765

Received 16 May 2007; accepted 20 July 2007
DOI 10.1002/app.27174
Published online 10 October 2007 in Wiley InterScience (www.interscience.wiley.com).

ABSTRACT: The inelastic deformation behavior of BMI-5250-4 neat resin, a high-temperature polymer, was investigated at 191°C. The effects of loading rate on monotonic stress–strain behavior as well as the effect of prior stress rate on creep behavior were explored. Positive nonlinear rate sensitivity was observed in monotonic loading. Creep response was found to be significantly influenced by prior stress rate. Effect of loading history on creep was studied in stepwise creep tests, where specimens were subjected to a constant stress rate loading followed by unloading to zero stress with intermittent creep periods during both loading and unloading. The strain-time behavior was strongly influenced by prior deformation history. Negative creep was observed on the unloading path. In addition, the behavior of the material was characterized in terms of a nonlinear viscoelastic model by means of creep and recovery tests at 191°C. The model was employed to predict the response of the material under monotonic loading/unloading and multi-step load histories. © 2007 Wiley Periodicals, Inc. J Appl Polym Sci 107: 1378–1386, 2008

Key words: creep; rate dependence; high-temperature properties; nonlinear response; viscoelasticity

INTRODUCTION

Thermosetting polymers are widely used as matrix materials in fiber-reinforced composites in a broad range of applications, including aerospace, automotive, and oil and gas industries.[1] The growing interest in the use of polymer matrix composites in critical load-bearing structures mandates extensive knowledge of the mechanical behavior as well as of the durability of these materials. To analyze or predict the behavior of the composite material, it is necessary to evaluate the contribution of the polymer matrix to the overall response of the composite. Generally, the linear viscoelastic behavior of polymers is readily accounted for when analyzing their short and long-term performance. However, the assumption of linearity is often used even when nonlinear behavior is evident because the nonlinearities are not well understood and useful experimental and theoretical means for nonlinear viscoelastic characterization and analysis are limited. Because of the revolutionary growth of computing power and development of advanced finite element software that allows for user defined material models, the computational aspect no longer impedes the progress in accounting for nonlinear viscoelastic response of polymers.[2,3] Instead, the focus has shifted to experimental and realistic theoretical characterization of the mechanical behavior of polymers.[4]

Several types of constitutive models developed to represent the mechanical behavior of polymeric materials employ the concept of the ''material clock'' to describe the dependence of relaxation rates on the state of the polymer. In these clock models, the nonlinear behavior is introduced and accounted for in terms of the free volume,[5,6] entropy,[7] stress,[8] or strain,[9] just as the WLF shift factor[10] defines the dependence of the relaxation rates on temperature. These constitutive models can generally be divided into two categories—differential and integral formulations. An extensive review of constitutive modeling of polymers is given elsewhere.[4,11–13] Among the integral formulations for viscoelastic materials, the free volume theory of Knauss and Emri[6] and the thermodynamically based model of Schapery[8] are well known and often used. This type of integral formulation, especially Schapery's model, is convenient for stress and strain analysis. Furthermore, the experimental data needed to determine the model parameters can be readily obtained from the relatively simple creep and recovery tests.

The BMI-5250-4 resin is widely used as a matrix material in aerospace composites because of its

The views expressed are those of the authors and do not reflect the official policy or position of the United States Air Force, Department of Defense or the U. S. Government.

Correspondence to: M. B. Ruggles-Wrenn (marina.ruggles-wrenn@afit.edu).

Contract grant sponsor: Air Force Office of Scientific Research (Dr. Charles Lee, Program Manager).

superior mechanical properties at high temperatures.[14] Developed specifically for the resin transfer molding process, the cross linked BMI-5250-4 resin reaches very low viscosity during transfer and maintains a low viscosity for a considerable time, allowing for fabrication of complex parts. The BMI-5250-4 based composites are capable of service temperatures up to 204°C. This study considers the time-dependent mechanical response of BMI-5250-4 neat resin at 191°C. The objective is to establish several qualitative features of the deformation behavior from experimental results and then to evaluate the ability of a nonlinear viscoelastic model to represent the observed inelastic behaviors. Discriminating tests investigating rate-dependence of the monotonic loading/unloading behavior as well as the influence of prior loading rate on recovery at zero stress and on creep response were carried out. In addition, piecewise linear deformation history, which involves stress-controlled tensile loading and unloading with intermittent periods of creep during loading and during unloading was used to explore the creep response on the loading and unloading paths. The nonlinear viscoelastic model of Schapery[8] was characterized by means of creep and recovery tests. The ability of the model to account for the observed nonlinear rate-dependent phenomena and to describe a complex loading history is assessed by comparing model predictions with the test data.

MATERIAL AND EXPERIMENTAL ARRANGEMENTS

The material used in this study was 5250-4 bismaleimide (BMI 5250-4) solid polymer. Cytec Engineered Materials Technical Services supplied the raw material. The neat resin panels were molded and cured at the Air Force Research Laboratory Materials and Manufacturing Directorate. A detailed description of the cure cycle is given elsewhere.[15] The molded panels were of dimensions 150 mm × 300 mm × 3.3 mm. The outer 10-mm-wide edges of the panels were discarded, and dog bone shaped specimens of 130-mm total length with a 7.6-mm-wide gage section were cut from the remainder of each panel. Elastic properties were established in tension tests to failure conducted in displacement control at the rate of 0.025 mm/s at 23 and 191°C. At 23°C the average stiffness was 4.40 GPa and the average strength, 102 MPa. At 191°C the average stiffness and strength were 2.85 GPa and 65 MPa, respectively.

A servocontrolled MTS mechanical testing machine equipped with hydraulic water-cooled collet grips, a compact resistance-heated furnace, and a temperature controller were used in all tests. An MTS TestStar II digital controller was employed for input signal generation and data acquisition. Strain measurement was accomplished with an MTS high-temperature air-cooled uniaxial extensometer. For elevated temperature testing, thermocouples were attached to the specimens using Kapton Tape to calibrate the furnace on a periodic basis. The furnace controller (using a noncontacting thermocouple exposed to the ambient environment near the test specimen) was adjusted to determine the power setting needed to achieve the desired temperature of the test specimen. The determined power setting was then used in actual tests. Thermocouples were not bonded to the test specimens after the furnace was calibrated.

All tests were performed in laboratory air environment. In all elevated temperature tests, a specimen was heated to 191°C at the rate of 1.5°C/min, and held at 191°C for additional 90 min prior to testing.

EXPERIMENTAL OBSERVATIONS

Monotonic stress-strain behavior—influence of loading rate

Effect of loading rate was explored in loading/unloading tests conducted with constant stress rate magnitudes of 1.0 and 0.01 MPa s^{-1} at 191°C. Results are presented in Figure 1. Note that the stress–strain curves do not exhibit a distinct linear range; the slope continues to decrease slowly with increasing stress. The stress–strain curves obtained at different stress rates show little if any dependence on rate leaving the origin. However, as the stress continues to increase a nonlinear effect of loading rate becomes apparent. A change in the stress rate by two orders of magnitude causes a much smaller change in strain; at 45 MPa the strains produced at the stress rates of 1.00 and 0.01 MPa s^{-1} are 1.7 and 2.1%, respectively. The unloading behavior is nearly linear. Inelastic strain measured immediately after reaching zero stress increases with decreasing stress rate. Note that

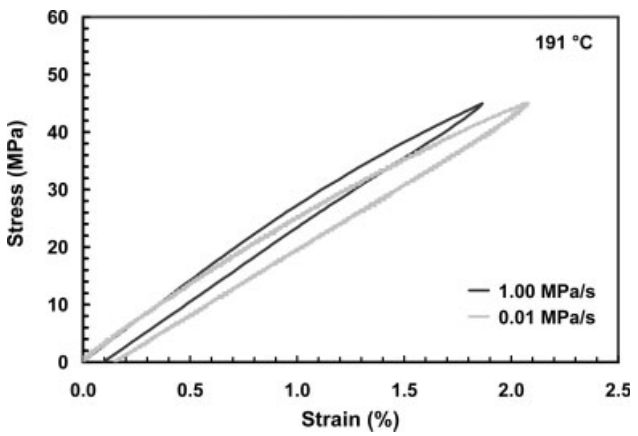

Figure 1 The influence of loading rate on the loading and unloading behavior of BMI-5250-4 neat resin at 191°C.

all inelastic strains measured upon unloading are <0.2%. Once the zero stress was reached, the load was controlled to stay at zero to observe the subsequent strain recovery. The inelastic strains measured upon unloading were fully recovered in both tests. In the test conducted with the stress rate magnitude of 1.0 MPa s^{-1}, the inelastic strain of 0.1% was recovered after mere 45 s. Conversely in the 0.01 MPa s^{-1} test, a much longer time of 0.5 h was required to recover 0.1% strain, and the inelastic strain of 0.15% measured upon unloading was fully recovered only after 1.5 h. The dramatically different time periods required to recover similar strains reveal that the recovery depends on the preceding stress rate and that the rate of recovery decreases with decreasing prior stress rate magnitude.

Creep behavior—influence of prior stress rate

Effect of prior stress rate on creep behavior was explored in creep tests preceded by uninterrupted loading to a target creep stress of 45 MPa at 1.0 and 0.01 MPa s^{-1}. Results in Figure 2 demonstrate that the creep behavior is profoundly influenced by the prior stress rate. For a given stress level, creep strain accumulation increases nonlinearly with increasing prior stress rate. An increase of two orders of magnitude in prior stress rate results in a nearly twofold increase in creep strain. The amount of creep strain for a given hold time does not depend on the stress alone. Therefore it is not sufficient to merely state a stress level when presenting creep results, prior stress rate must be accounted for as well.

Creep behavior—influence of prior loading history

The effect of prior loading history on creep response was studied in stepwise creep tests, schematically shown in Figure 3. Loading/unloading was performed in stress control with the stress rate magnitude of 1.0 MPa s^{-1}. Creep periods of 1 h duration were introduced at 30 and 40 MPa during both loading and unloading and at the maximum stress of 45 MPa. Immediately after unloading to zero stress (load), the specimen was allowed to recover at zero stress for 16 h.

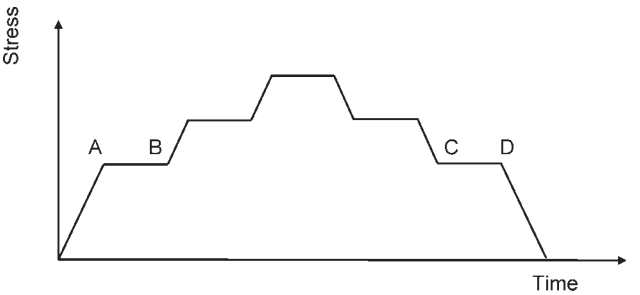

Figure 3 Schematic illustrating the control (input) signal in the stress-controlled loading-unloading test with intermittent periods of creep. Segments AB and CD represent creep tests of equal duration conducted at the same creep stress level. Creep test AB is performed during loading, while creep test CD is performed during unloading.

A typical stress–strain curve obtained in a stepwise creep test is shown in Figure 4. The creep strain vs. time curves pertaining to this test are presented in Figure 5. It is seen that in creep tests performed on the loading stress–strain path, the creep rate and the creep strain accumulation decrease despite an increase in creep stress. Larger creep strain is accumulated at 30 MPa than at the higher stresses of 40 and 45 MPa. It is noteworthy that in a sequence of creep tests it is possible to accumulate larger creep strain at a lower creep stress level. While this behavior may appear anomalous, it has been previously observed at room temperature and reported for

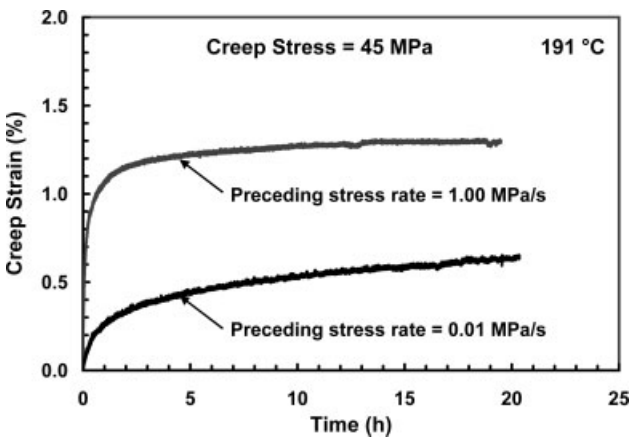

Figure 2 Creep strain vs. time at 45 MPa and 191°C. Effect of prior stress rate on creep strain is apparent. Creep strain increases nonlinearly with prior loading rate.

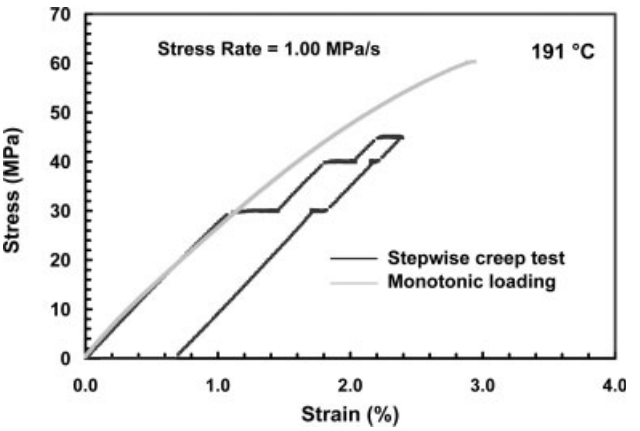

Figure 4 Stress controlled test with intermittent creep periods of 3600 s duration at 191°C. At the same stress level the creep rate is different during loading and unloading. Light gray line (—) is the uninterrupted stress–strain curve.

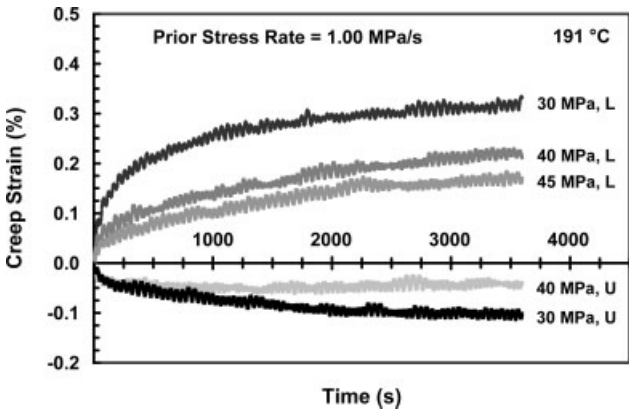

Figure 5 Creep curves pertaining to the stepwise creep test shown in Figure 4. All creep is primary. L, loading; U, unloading.

Nylon 66[16] and polyphenylene oxide.[17] Furthermore, Krempl and Bordonaro[16] and Khan[17] explain this seemingly unusual phenomenon in the context of the viscoplasticity theory based on overstress (VBO)[18,19] and demonstrate that VBO is capable of representing it. While it is not necessary to reproduce the VBO formulation here, it is instructive to consider the current experimental results within the VBO framework, where the inelastic rate of deformation depends on the overstress. To speculate on the evolution of the overstress in the stepwise creep test, we compare the stress–strain curve obtained in this test with an uninterrupted stress–strain curve obtained at the same stress rate (the light gray line in Fig. 5). The first creep test performed at 30 MPa results in ≈0.34 % strain accumulation, which places the stress–strain curve ~ 7 MPa below the uninterrupted curve at the end of the creep period. At the conclusion of the 30 MPa creep test, stress rate controlled loading resumes, but does not continue long enough to allow the stress–strain curve to reach the uninterrupted curve. After the 40 MPa creep period, the stress–strain curve falls further below the uninterrupted curve (light gray line). In the context of the VBO, this indicates that the overstress (which is directly responsible for inelastic deformation) is higher at the start of the 30 MPa creep test than at the start of the 40 or the 45 MPa creep periods. The higher overstress results in higher creep strain rates and higher strain accumulations.

In creep tests performed during unloading, negative creep rates are observed, strain decreases with time. For a given creep stress and time, creep response is different in magnitude and in form on loading and on unloading. In addition to differences in creep strain accumulation, the rate of change of strain changes sign when a creep test is performed on the unloading path. As the creep stress level decreases, the average creep rate magnitude increases and negative creep becomes more pronounced. A larger decrease in strain is observed at 30 MPa than at 40 MPa. Negative creep on unloading was also reported for nylon 66,[16] for polycarbonate, high density polyethylene and polyphenylene oxide,[17] as well as for unplasticized PVC plastic[20] and rigid polyurethane foam.[21]

To further illuminate effects of prior deformation history on creep, results of the 45 MPa creep period from the stepwise creep test are compared with those of the creep test preceded by uninterrupted loading (at the same stress rate) to 45 MPa (Fig. 6). A significant difference in creep response is apparent. Creep strain accumulated in the creep test preceded by uninterrupted loading is nearly five times that obtained in the stepwise creep test. In the context of the VBO, the overstress at the start of the 45 MPa creep period in the stepwise test is considerably lower than that at the 45 MPa point in the monotonic stress–strain curve, resulting in lower creep rate and creep strain.

Results obtained during the 16-h recovery period following unloading to zero stress at the conclusion of the stepwise creep test are shown in Figure 7. Note that Figure 7 includes a prediction obtained using a nonlinear viscoelastic model, which is discussed in the subsequent section. It is seen that a full recovery observed in the loading/unloading test conducted at the same constant stress rate magnitude is not achieved in this case. Inelastic strain of 0.67% measured immediately upon unloading to zero stress is only partially recovered after 16 h. Furthermore, results in Figure 7 reveal that the recovery is nearly saturated after 10 h; only negligible amount of strain is recovered after that. Considering the near zero recovery rate observed for the recovery time 10 h $< t_R <$ 16 h, it is unlikely that the full recovery

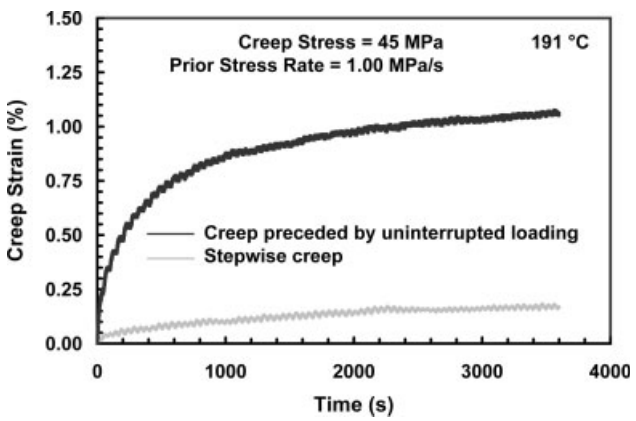

Figure 6 Creep curves obtained at 45 MPa in a stepwise creep test and a creep test preceded by uninterrupted loading. Strains at the beginning of creep tests are 1.71% (creep preceded by uninterrupted loading) and 2.23% (stepwise creep).

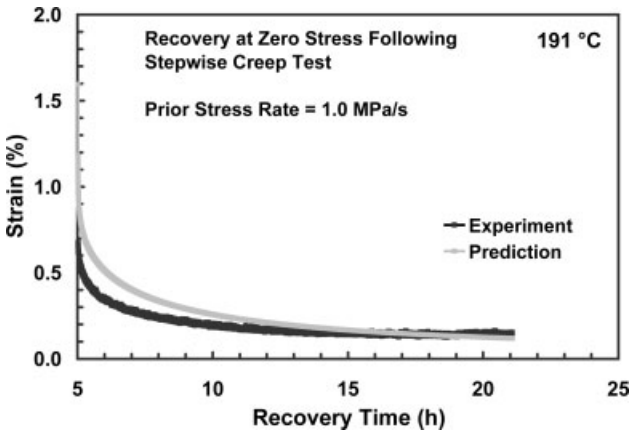

Figure 7 Recovery at zero stress following the stepwise creep test conducted with the stress rate magnitude of 1.0 MPa s^{-1}. A comparison between experimental data and predicted stain response.

would be achieved even if a much longer time period were allowed.

MODELING

Nonlinear viscoelastic model—characterization

The behavior of the BMI-5250-4 neat resin at 191°C was also characterized in terms of the nonlinear viscoelastic model of Schapery.[8,22] The model is based on general thermodynamic principles and offers the advantage of retaining the single time integral form in the nonlinear range. The nonlinear effects are expressed by means of the stress-dependent material functions.

For uniaxial loading the stress–strain relation reduces to:

$$\varepsilon(t) = g_0 D(0)\sigma + g_1 \int_0^t \Delta D(\psi - \psi') \frac{dg_2\sigma}{d\tau} d\tau \qquad (1)$$

Here $D(0)$ is the initial component of the creep compliance, $\Delta D(\psi)$ is the transient component of compliance represented by a power law

$$\Delta D(\psi) = C\psi^n, \qquad (2)$$

ψ is the reduced time given by

$$\psi = \psi(t) = \int_0^t \frac{dt'}{a_\sigma[\sigma(t')]}; \quad \psi' = \psi(\tau) = \int_0^\tau \frac{dt'}{a_\sigma[\sigma(t')]}, \quad (3)$$

and g_0, g_1, g_2, and a_σ are the stress-dependent material functions.

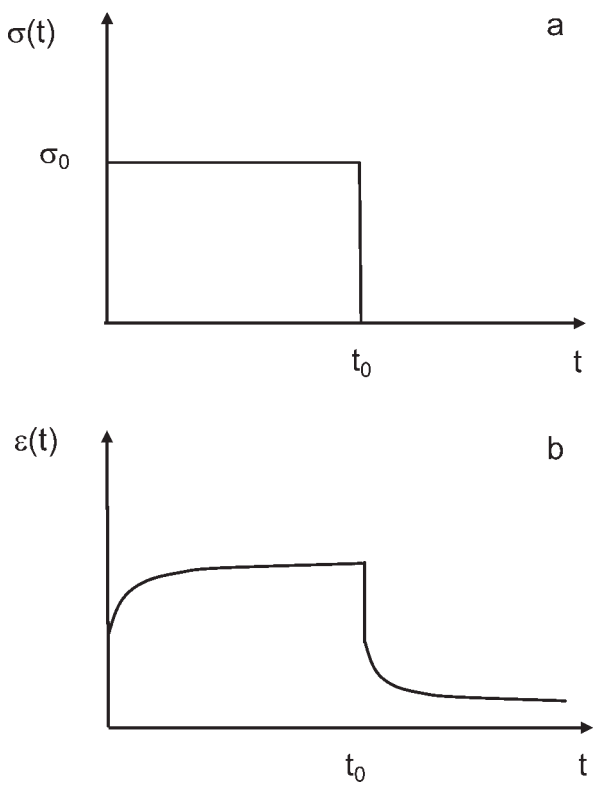

Figure 8 Schematic of stress input for a creep and recovery test (a) and the associated strain response (b).

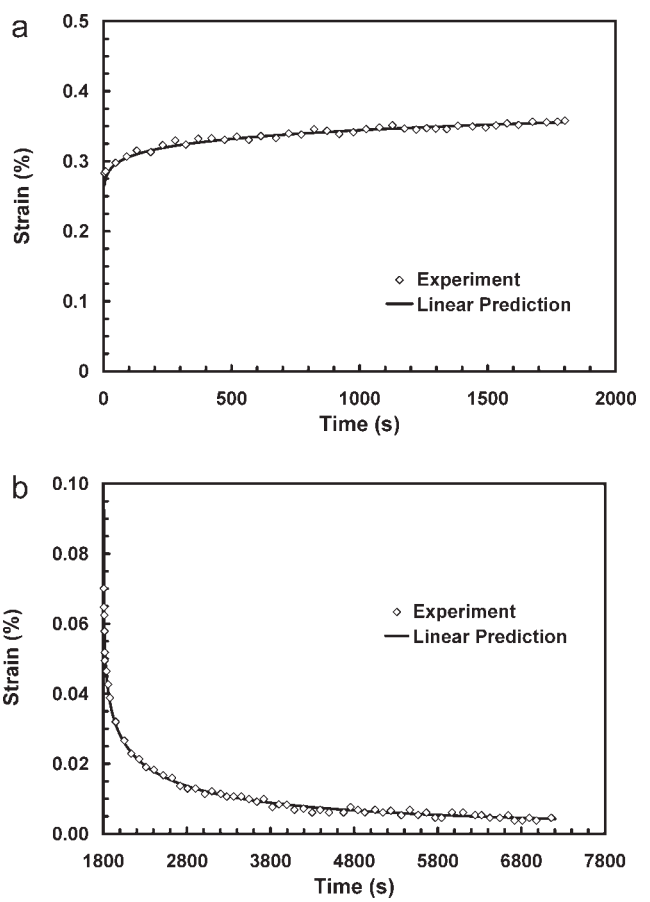

Figure 9 Comparison between the linear prediction and experiment {σ_o = 8 MPa} for: (a) creep and (b) recovery.

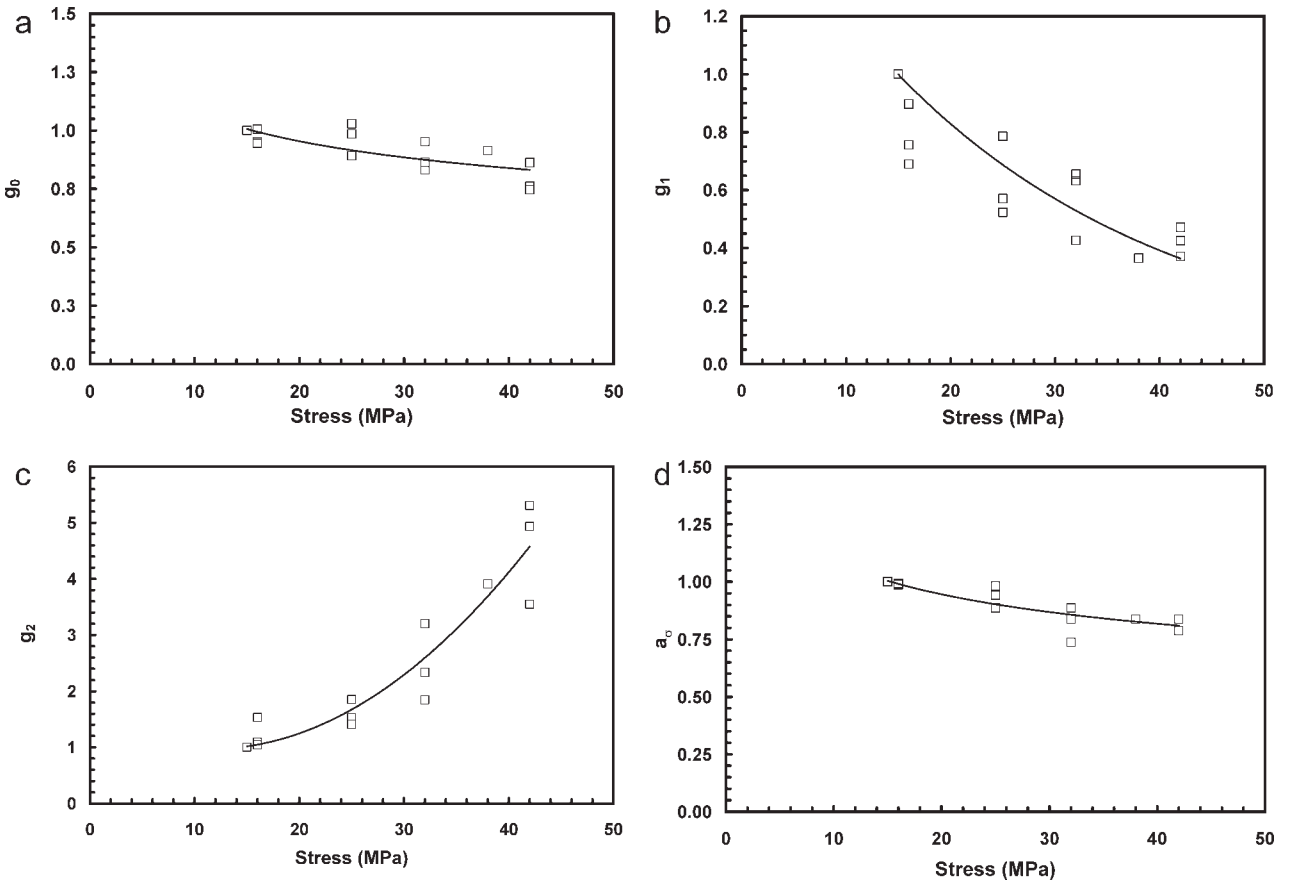

Figure 10 Material properties as functions of stress in the nonlinear range: (a) g_0 vs. stress, (b) g_1 vs. stress, (c) g_2 vs. stress, (d) a_σ vs. stress.

The material properties in eqs. (1)–(3) were obtained from uniaxial creep and recovery tests involving the application of a single step stress of magnitude σ_0 and its removal after duration t_0, as depicted in Figure 8(a). The associated strain response shown in Figure 8(b) was recorded for durations exceeding $3t_0$. The stress level magnitudes σ_0 were 8, 16, 25, 32, and 42 MPa. Creep time t_0 was 30 min. Recovery time was 90 min in the 8 MPa test and 300 min in all other tests. Note that loading and unloading could not be realized in the step fashion depicted in Figure 8(a). In reality, loading and unloading were applied at a constant rate of 3 MPa s^{-1}, requiring less than 15 s to attain the prescribed stress levels. Three tests were conducted for each stress level magnitude σ_0 at 191°C.

The range of the linear viscoelastic response, where creep strain is proportional to the applied stress σ_0 and a complete recovery is achieved upon load removal, was determined experimentally to occur when $0 < \sigma_0 \leq 15$ MPa. Following established procedures,[23,24] it was possible to express the creep and recovery data obtained within the linear range in a power-law form as follows:

$$\varepsilon(t) = \begin{cases} (D_0 + D_1 t^n)\sigma_0 & 0 < t < t_0 \\ D_1[t^n - (t - t_0)^n]\sigma_0 & t > t_0 \end{cases} \quad \sigma_0 \leq 15\text{MPa}, \tag{4}$$

A comparison of Eq. (4) with experimental data in the linear range is presented in Figure 9. Recognizing that in the linear viscoelastic case $g_0 = g_1 = g_2 = a_\sigma = 1$, the values of the three constants $D(0) = D_0$, $C = D_1$, and n could be determined. Accordingly, the following properties were obtained from experimental data in the linear range ($\sigma_0 \leq 15$ MPa): $D(0) = 28.9 \times 10^{-5}$ MPa^{-1}, $C = 6.05 \times 10^{-5}$ MPa^{-1} s^{-n}, $n = 0.11$, where time t is in seconds. Using creep and recovery data in the nonlinear range, the material properties g_0, g_1, g_2, and a_σ were established as the functions of stress. The results are presented in Figure 10. On the basis of these results the material functions g_0, g_1, g_2, and a_σ can be expressed as follows:

$$a_\sigma = 1.7711\sigma^{-0.2094}, \quad g_0 = 1.6636\sigma^{-0.1857},$$
$$g_1 = 1.7500e^{-0.0374\sigma}, \quad g_2 = 0.0039\sigma^2 - 0.0906\sigma + 1.50. \tag{5}$$

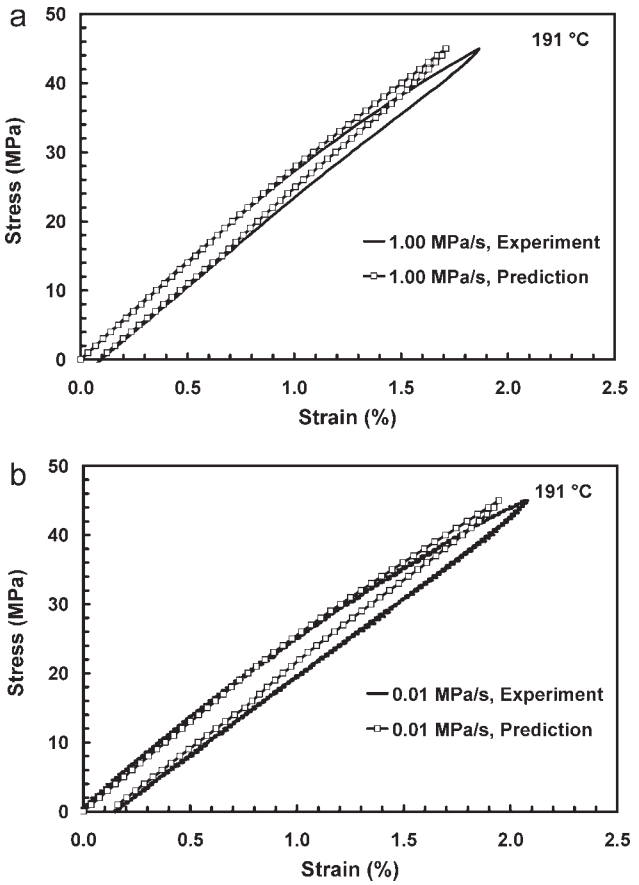

Figure 11 A comparison between experimental and predicted stress–strain curves for BMI-5250-4 neat resin at 191°C at constant stress rates of: (a) 1.0 MPa s^{-1} and (b) 0.01 MPa s^{-1}.

Model evaluation

The model capabilities were assessed by comparing the predictions with experimental results obtained in tests that differ in kind from the creep and recovery experiments used for model characterization. Predictions of the loading/unloading tests conducted with the constant stress rate magnitudes of 1.0 and 0.01 MPa s^{-1} are shown together with the experimental data in Figures 11(a) and 11(b), respectively. It is seen that the model successfully accounts for the effect of loading rate; larger strains are produced at a lower stress rate. Yet while the qualitative predictions are fairly good, the model under-predicts the strains at stresses above 20 MPa for both loading rates.

Figures 12(a) and 12(b) show the strain-time responses obtained in the 30 MPa creep tests preceded by uninterrupted loading at the rates of 1.0 and 0.01 MPa s^{-1}, respectively, together with model predictions. Two different stress paths were used for calculating the predicted strain response: (1) the full path, where the stress was increased to 30 MPa at a constant stress rate used in experiment and (2) the step path, where the stress of 30 MPa was applied as a step function. In the case of the prior stress rate of 1.0 MPa s^{-1}, the predicted strain response is in good agreement with the experimental data. Note that the same strain response is predicted for both stress paths and both predictions correlate well with experiment. This is hardly surprising, considering that the stress rate of 1.0 MPa s^{-1} is of the same order of magnitude as that used in the creep and recovery characterization experiments. Conversely, strain responses predicted for the prior stress rate of 0.01 MPa s^{-1} fall noticeably above the experimental data [see Fig. 12(b)]. While using the full stress path improves prediction of the strain at the start of the creep test, predicted creep strain exceeds the experimental data and converges with the creep strain predicted for the step stress path. The model does not account for the effect of prior stress rate on creep, essentially the same creep strain response is predicted for the two significantly different prior stress rates.

Stepwise creep test conducted with the loading/unloading stress rate magnitude of 1.0 MPa s^{-1} was also used for model evaluation. Figures 13(a) and 13(b) show comparison between experimental and predicted creep curves obtained on the loading and

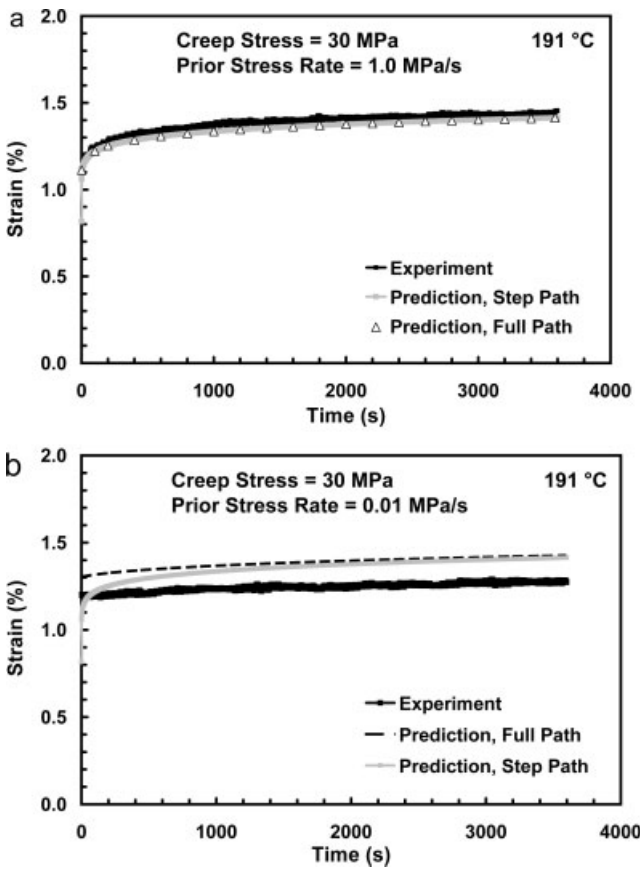

Figure 12 A comparison between experimental and predicted creep curves obtained for BMI-5250-4 neat resin at 30 MPa and 191°C for the prior loading rate of (a) 1.0 MPa s^{-1} and (b) 0.01 MPa s^{-1}.

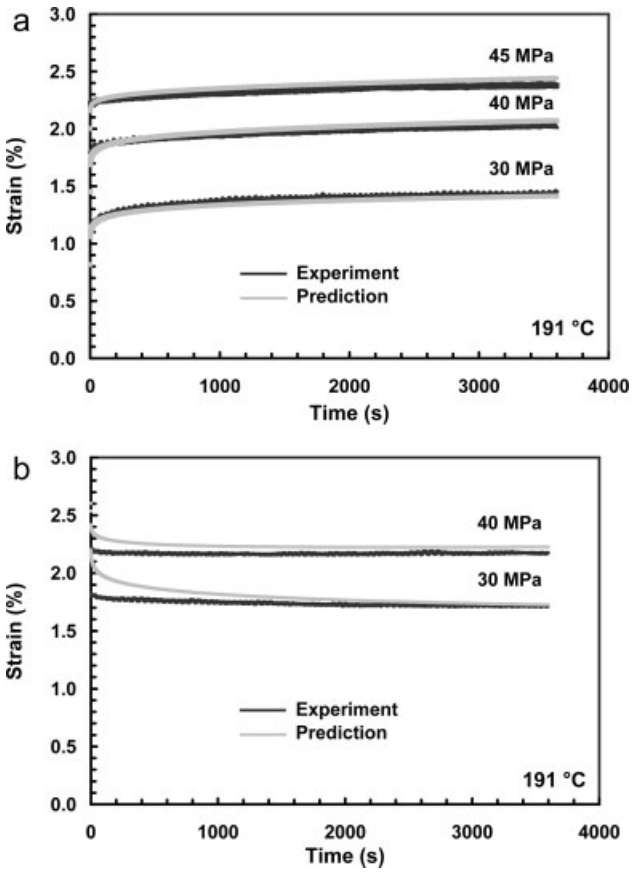

Figure 13 A comparison between experimental and predicted creep curves obtained on (a) the loading path and (b) the unloading path of the stepwise creep test conducted with the stress rate magnitude of 1.0 MPa s^{-1}.

on the unloading paths, respectively. It is seen that the model successfully predicts creep response during loading. Predictions of the creep response at 40 and 30 MPa during unloading are satisfactory. While for both creep stress levels, the predicted strains considerably exceed the experimental values at the start of the creep test, predictions are reasonably close to experimental data for creep times $t_C > 1000$ s. However, model prediction for the recovery at zero stress following the stepwise creep test is less satisfactory (see Fig. 7). The model over-predicts strain at the beginning of the recovery period. Moreover, while for the recovery times 5 h $< t_R <$ 16 h prediction agrees fairly well with experiment, the model predicts a higher recovery rate than that observed in the test. Contrary to experimental observations, the model predicts that full recovery would be achieved after $\sim$ 350 h.

CONCLUDING REMARKS

Effect of loading rate

Effect of loading rate was explored in loading/unloading tests conducted with constant stress rates of 1.0 and 0.01 MPa s^{-1} at 191°C. The BMI-5250-4 neat resin exhibits nonlinear rate sensitivity at 191°C. The unloading stress–strain behavior is nearly linear. Inelastic strain measured immediately after reaching zero stress increases with decreasing prior loading rate magnitude. Inelastic strains measured after loading to 45 MPa and unloading to zero stress are fully recovered regardless of the loading/unloading rate. However, the rate of recovery increases significantly with increasing prior loading rate magnitude.

Effect of prior stress rate on creep behavior was explored in creep tests at 45 MPa preceded by loading to the creep stress level at the constant stress rates of 1.0 and 0.01 MPa s^{-1}. Creep response is significantly affected by the prior stress rate. Creep strain accumulation at a given creep stress increases nonlinearly with increasing prior stress rate.

Effect of prior loading history

Effect of prior loading history on creep behavior was explored in stepwise creep tests incorporating loading and unloading with intermittent creep periods at several stress levels. Creep response is profoundly influenced by prior loading history. In a sequence of creep tests, it is possible to accumulate greater creep strain at a lower stress level. For a given creep stress and time, creep response is different in magnitude and in form when a creep test is conducted during loading and unloading. Negative creep (i.e., a decrease in strain) is observed during unloading, which becomes more pronounced as the creep stress decreases.

Nonlinear viscoelastic modeling

The nonlinear viscoelastic model of Schapery was characterized and evaluated. It is found that the model is generally capable of predicting the nonlinear behavior of the BMI-5250-4 polymer resin at 191°C. However some limitations were identified. The model qualitatively reproduced the loading and unloading stress–strain behavior at constant stress rates. The model cannot account for the effect of prior loading rate on creep response. The model predicts the same creep stain response for the prior loading rates, which differ by two orders of magnitude. This prediction is excellent provided loading to creep stress occurs at a sufficiently fast rate (≥1.0 MPa s^{-1}). For the slower prior stress rate of 0.01 MPa s^{-1}, the prediction is poor. The model is capable of representing effects of prior deformation history on creep response. Predictions of creep strains that occur during loading are excellent. The model successfully predicts negative creep observed on the unloading path, although predictions are less accurate. The model predicts a strain recovery at zero

stress following the stepwise creep test, but overestimates the recovery rate.

The authors would like to thank Dr. Y. J. Weitsman for many valuable discussions.

References

1. NASA/Glenn Research Center. DMBZ Polyimides Provide an Alternative to PMR-15 for High-Temperature Applications; NASA/Glenn Research Center, 2005.
2. Ellyin, F.; Xia, Z. J Eng Mater Technol 2006, 128, 579.
3. Shaw, S.; Warby, M. K.; Whiteman, J. R. An Introduction to the Theory and Numerical Analysis of Viscoelasticity Problems; Brunel University: England, 1997.
4. Schapery, R. A. Int J Solids Struct 2000, 37, 359.
5. Losi, G. U.; Knauss, W. G. Polym Eng Sci 1992, 32, 542.
6. Knauss, W. G.; Emri, I. Polym Eng Sci 1987, 27, 86.
7. Shay, R. M., Caruthers, J. M. Polym Eng Sci 1990, 30, 1266.
8. Schapery, R. A. Polym Eng Sci 1969, 9, 295.
9. O'Connell, A.; McKenna, G. B. Mech Time-Depend Mater 2002, 6, 207.
10. Williams, M. L.; Landel, R. F.; Ferry, J. D. J Am Chem Soc 1955, 77, 3701.
11. Xia, Z.; Shen, X.; Ellyin, F. Mech Time-Depend Mater 2006, 9, 281.
12. Popelar, C. F.; Liechti, K. M. Mech Time-Depend Mater 2003, 7, 89.
13. Lustig, S. R.; Shay, R. M.; Caruthers, J. M. J Rheol 1996, 40, 69.
14. Morgan, R. J.; Shin, E. E.; Lincoln, J.; Zou, J. SAMPE J 2001, 37, 102.
15. Pagano, N. J.; Schoeppner, G. A.; Kim, R.; Abrams, F. L. Compos Sci Technol 1998, 58, 1811.
16. Krempl, E.; Bordonaro, C. M. Polym Eng Sci 1995, 35, 310.
17. Khan, F. J. PhD Dissertation; Rensselaer Polytechnic Institute: Troy NY, 2003.
18. Krempl, E. Unified Constitutive Laws of Plastic Deformation; Academic Press: San Diego, 1996, p 281.
19. Ho, K.; Krempl, E. Int J Plast 2000, 18, 851.
20. Onaran, K.; Findley, W. N. J Appl Mech E 1971, 38, 30.
21. Lai, J. S. Y.; Findley, W. N. Trans Soc Rheol 1973, 17, 129.
22. Lou, Y. C.; Schapery, R. A. J Compos Mater 1971, 5, 208.
23. Jerina, K. L.; Schapery, R. A.; Tung, R. W.; Sanders, B. A. Short Fiber Reinforced Composite Materials, ASTM STP 772; ASTM 1982, p 225.
24. Peretz, D.; Weitsman, Y. J. J Rheol 1982, 26, 245.